Mechanical properties of aerogel composites for casting purposes

LORENZ RATKE*, SABINE BRÜCK
Institute of Space Simulation, German Aerospace Center DLR, 51140, Köln
E-mail: lorens.ratke@dlr.de

Published online: 4 February 2006

Polymeric aerogels are used in this study to bind foundry sand forming thus a new kind of mould and core material called AeroSand. A core and mould material in general shall be able to withstand all handling stresses in a foundry shop, withstand the thermal and mechanical stresses exerted onto them during casting, but should also easy removable from a casting. Therefore mechanical properties are important besides others and this paper therefore concentrates on bending and compression strength of AeroSands. It is shown that the strength levels obtainable with aerogel binders are comparable to conventional binder systems. One essential advantage of AeroSands, namely the easy core removal, is not payed off by a loss in strength. The mechanical properties can be explained using a simple extension of the Griffith criterion taking into account the microstructure of the sand aerogel composite and the fracture path.

1. Introduction

Composites made from conventional foundry sands and polymeric aerogels are in discussion as a new type of mould and core material for general casting applications [1–4]. Binding sand grains not with resins like epoxy, polyurethan or furan but with a polymeric aerogel is a quite new approach and opens new possibilities, since the binder itself is nano-structured, open porous, has an extremely high internal surface and closes the large pores made by the sand grains. Therefore we observed that e.g. aerogel bonded sands, so-called AeroSands, can easily be thermally disintegrated in air at temperatures above 350°C without leaving any residue on the sand surface. This allows prepare casting cores with complex geometries since core removal is very easy and perfect without any mechanical effort. The huge internal surface allows to use the AeroSand itself as a raiser, since it adsorbs completely all gases evolving during casting.

The application of AeroSands in foundry practice, however, depends strongly on their mechanical properties. The core and mould material shall be able to withstand all handling stresses in a foundry shop, withstand the thermal and mechanical stresses exerted onto them during casting. Therefore we investigated the mechanical properties of the new type of mould and core material and describe the experimental observation with a modified Griffith criterion for brittle solids taking into account the fracture path and the special porous nature of the material.

2. Experimental procedures

2.1. Preparation of AeroSands

Aerogel composites were prepared from a mixsture of foundry sands and a polymeric aerogel solution. The aerogel solution was prepared from a mixture of resorcinol (Merck), Formaldehyd (37% solution from Merck), deionized water and sodiumbicarbonate as a catalyst. The details of aerogel production are described in [3, 5]. After mixing the components a clear solution is obtained which gels within 24 h at 40°C and can then be dried at ambient conditions in 24 h. With respect to the current context it is important to notice that the solution of resorcinol, formaldehyde and water has initially a pH value of 6. The addition of sodiumbicarbonate changes the pH value from acidic towards base values, depending on the amount added. The more catalyst is added the smaller the particle size of the aerogel network becomes and the larger the pore volume. Fricke and co-workers [7] have shown that only for ratio of resorcinol (R) to catalyst (C) above 1000 RF aerogels can be dried at ambient conditions. For R/C values smaller and thus shifting the pH value to larger values supercritical drying is necessary.

*Author to whom all correspondence should be addressed.
0022-2461
DOI: 10.1007/s10853-005-3152-8

The composites were prepared by filling aluminiumoxide sands, Alodur^{TM}, with three different grain size classes, silicon carbide sands from EKS, quartz sand (Quarzwerke Frechen) and hollow mullite spheres, E-spheres^{TM} from enviropsheres Ltd. of different size with varying amounts of the above solution. In order to prepare compact packed sand beds the sands were filled into a stainless steel vessel and the solution poured in with amounts of 4, 10, 16 and 24 wt% calculated with respect to the weight of the sand. The sand-solution mixture was then stirred with a Hobart mixer at slow stirring speeds. With low amounts of solution (less than 10%) the sand seems dry and could even be brought into form for testing using a core shooting machine, at higher amounts the mixture has the appearance of a slurry. The sand solutions mixtures were filled into cylindrical polycarbonate tubes (30 mm diameter, 50 mm length) which were closed to allow for gelation to take place without evaporation of the components. Gelation and drying was performed in a drying chamber at 40°C. For drying the tubes were opened. We observed that the sands accelerated gelation. Typical gelation times were reduced to a few hours and drying times also were shorter. For bending test the sand-solution mixtures were filled into steel forms having rectangular cavities with 25 × 25 mm cross section 150 mm length.

2.2. Testing of AeroSands

Critical test for mould and core materials are compression and especially bending tests [6]. We performed compression tests with the cylindrical samples and three point bending tests with the rectangular bars in an INSTRON 5 kN machine using a cross head speed of 1 mm/min. The span between the bearings was 130 mm, the radius of curvature of the counter bearings 3 mm and the central load applied through a cylinder with a radius of 20 mm. The force displacement or deflection curves were recorded and used to derive from them the elastic modulus. For each sand or RF aerogel content, sand grain size and sand type we tested three to five samples. The values for the compression or bending strength and elastic modulus given in the tables below are mean values. On the fracture surfaces we analysed in a SEM (Leica 1530 VP) the fracture path in order to reveal if the fracture takes place along the sand aerogel interface or within the aerogel. A typical bending stress-strain diagram is shown in Fig. 1, which was calculated from force-deflection curves using classical bending theory [9]. The stress plotted is the maximum tensile stress in the outer fibre, calculated from the bending moment and the second moment of area. The strain in the outer tensile fibre of the beam is calculated as the difference between its actual arc length l and the initial span of the bearings l_0 as $\epsilon = (l - l_0)/l_0$. The actual arc length can be calculated as a function of the deflection of the beam. Initially the stress-strain curve has a more parabolic appearance indicating the compliance of the whole system. This is followed by a linear increase of stress with strain until the stress suddenly drops indicating brittle fracture.

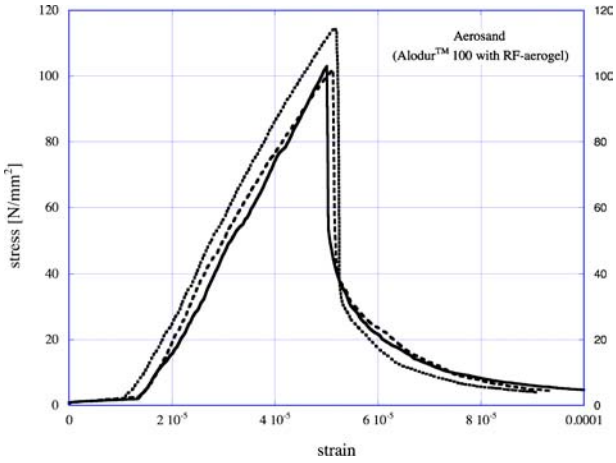

Figure 1 Examples of stress-strain diagrams measured with AeroSands made from Alodur^{TM} and RF-Aerogel.

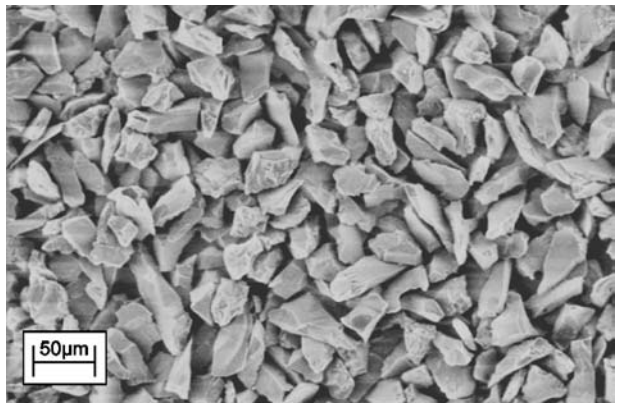

Figure 2 The Alodur^{TM} sand has a splintery appearance. The grain surfaces are rough.

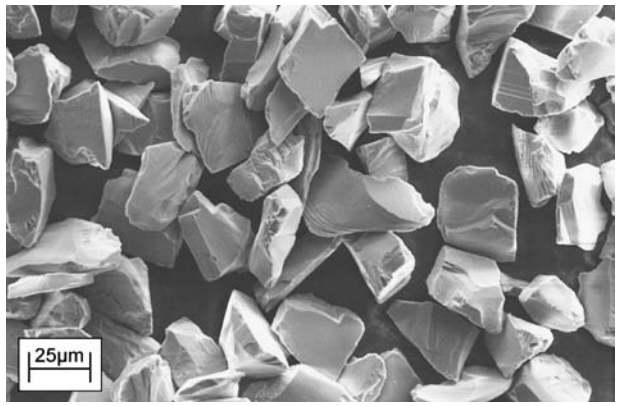

Figure 3 SEM picture of a SiC sand from EKS. Note that the SiC grains have a splintery appearance and are facetted at the surface exhibiting terraces, kinks and ledges.

3. Results

In order to understand the mechanical properties it is important to have a clear picture of the microstructure realized in these sand aerogel composites. The three sand

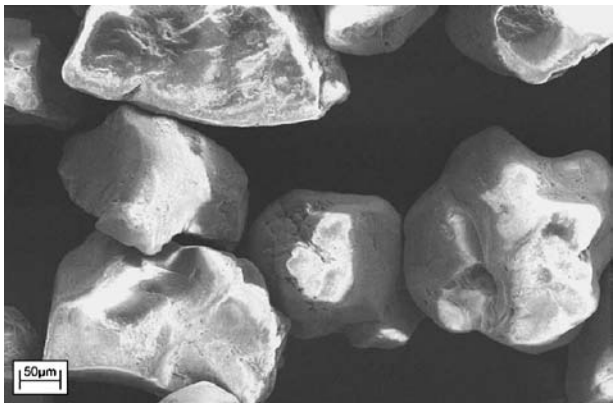

Figure 4 SEM picture of a quartz sand from Quarzwerke Frechen. The quarz sand grains have the shape of potatoes with rounded corners and edges.

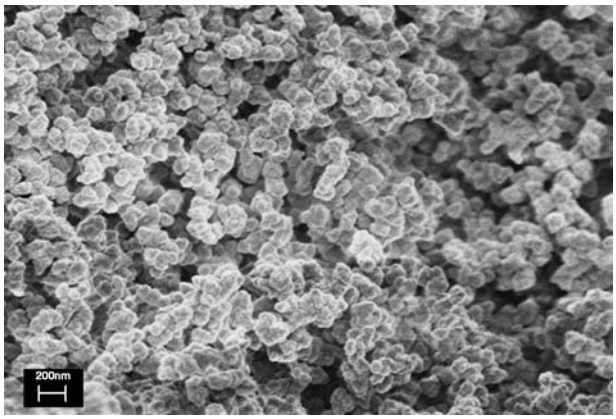

Figure 5 SEM picture of a fracture surface of a pure RF aerogel showing the network of particles building the aerogel structure. The polymeric particles building the aerogel have a typical diameter of around 50 nm.

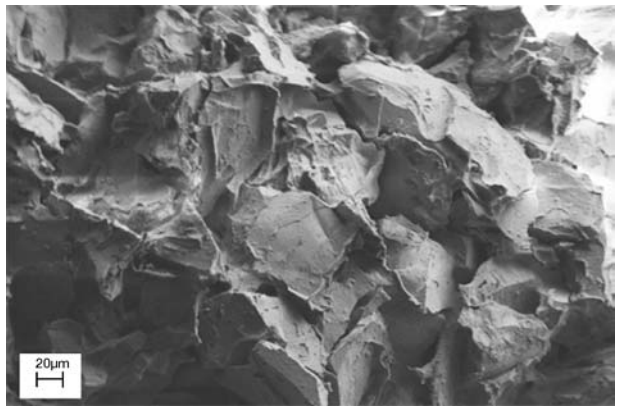

Figure 6 The fracture surface of an RF aerosand broken in a bending test shows that the fracture path followed the interfaces between the sand grains and the RF aerogel.

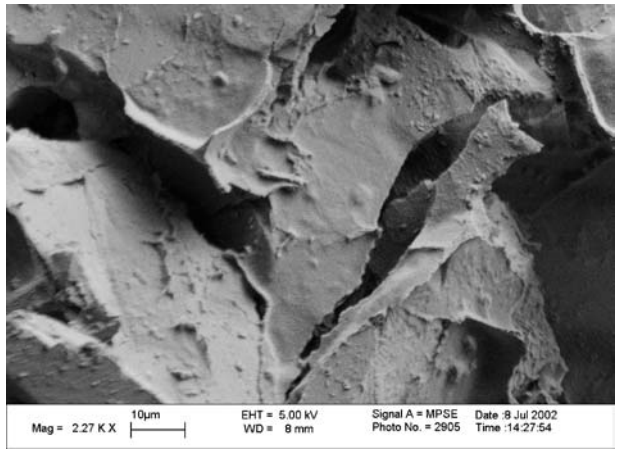

Figure 7 The same fracture surface as in Fig. 6 at higher magnification showing that the pore space between the sand grains was completely filled by the solution during preparation.

types used, namely Alodur^{TM}, which is mainly aluminiumoxide, silicon carbide, hollow spheres consisting of nearly stochiometric mullite (E-spheres^{TM}) and quartz sand show different grain morphologies. The e-spheres are mainly spherical hollow spheres with a smooth surface. Quartz grains have rounded edges and look more like potatoes. SiC is polyhedral in shape and their surface exhibits facets with ledges and kinks. Alodur^{TM} grains show a splintery appearance with a somehow rough surface.

The porous structure of the pure RF-aerogel is shown in Fig. 5. The aerogel consists of polymeric particles having approximately a size of 30 to 50 nm. The pore space in between these particles seems to be of the same order. Measurements showed that the RF aerogels typically have a density of 350 kg/m^3, meaning a porosity of around 70 vol.%.

The fracture surfaces of the bent specimen were looked at in the SEM. They all show the same type of fracture surface. The fracture path follows the interface between sand and aerogel and in between the sand grains the aerogel has fractured in a mode normal to the applied stress. Here it might be worth to note that measurements we performed with pure polymeric RF aerogels gave bending strengths in between 1 and 2 MPa, indicating that pure aerogels are fragile [10].

At high resolution the porous structure of the aerogel can be revealed, which is required to take up the casting gases evolving.

The results of the compression and bending tests are given in Tables I and II. Looking at the variation of the bending strength they all are in a range of around 1 MPa and 3 MPa. These values are comparable to those of a pure aerogel (1–2 MPa), but are larger at the highest amounts of aerogel used. Values larger than 2 MPa indicate that a firm bonding of the sand to the aerogel is achieved. Looking at other trends one recognizes that with decreasing RF aerogel fraction both strengths decrease. With decreasing grain size at constant RF aerogel fraction the strengths increase. It also is obvious that the highest values are obtained with SiC sands, followed by Alodur^{TM}, quartz and e-spheres^{TM}. It seems that there is first a relation to the grain morphology and surface and also that the bonding between the silicon oxide containing sands and the RF aerogel is worse compared to the other sands.

TABLE I Bending strength of various combinations of sands of different grain size with RF aerogel at different solution fractions. Alodur™ is a trademark of and e-spheres™ is a trademark of envirospheres Ltd.

RF sol fraction (wt%)	Grain size (μm)	Sand type	Bending strength (N/mm^2)
24	Alodur™	45–75	3.05
16	Alodur™	45–75	2.85
10	Alodur™	45–75	1.28
4	Alodur™	45–75	1.08
24	Alodur™	63–106	3.29
16	Alodur™	63–106	2.34
10	Alodur™	63–106	1.63
24	Alodur™	106–150	1.78
10	Alodur™	106–150	1.11
4	Alodur™	106–150	1.11
24	SiC	45–75	3.17
16	SiC	45–75	2.10
4	SiC	45–75	0.86
24	SiC	106–150	2.12
16	SiC	106–150	1.62
10	SiC	106–150	1.92
4	SiC	106–150	1.43
40	E-Spheres™	20–300	1.18
31	E-Spheres™	20–300	0.78
24	E-Spheres™	20–300	1.39
16	E-Spheres™	20–300	0.36
24	Quarz	63–250	1.10
16	Quarz	63–250	1.22
10	Quarz	63–250	1.29
4	Quarz	63–250	0.82

TABLE II Compression strength of various combinations of sands of different grain size with RF aerogel at different solution fractions. Alodur™ is a trademark of Munk+Schmitz and e-spheres™ is a trademark of envirospheres Ltd.

RF sol fraction (wt%)	Grain size (μm)	Sand type	Bending strength (N/mm^2)
24	Alodur™	45–75	10.14
16	Alodur™	45–75	4.96
10	Alodur™	45–75	4.58
4	Alodur™	45–75	5.54
24	Alodur™	63–106	8.6
16	Alodur™	63–106	8.24
10	Alodur™	63–106	6.19
4	Alodur™	63–106	3.38
24	Alodur™	90–125	6.46
16	Alodur™	90–125	6.41
10	Alodur™	90–125	3.97
24	Alodur™	106–150	4.34
16	Alodur™	106–150	2.15
10	Alodur™	106–150	2.04
4	Alodur™	106–150	0.65
24	SiC	45–75	10.08
16	SiC	45–75	6.39
10	SiC	45–75	4.47
4	SiC	45–75	1.51
31	E-Spheres™	20–300	1.48
24	E-Spheres™	20–300	0.89
16	E-Spheres™	20–300	0.56
10	E-Spheres™	20–300	0.44
24	Quarz	63–250	1.66
16	Quarz	63–250	1.77
10	Quarz	63–250	0.92
4	Quarz	63–250	0.78

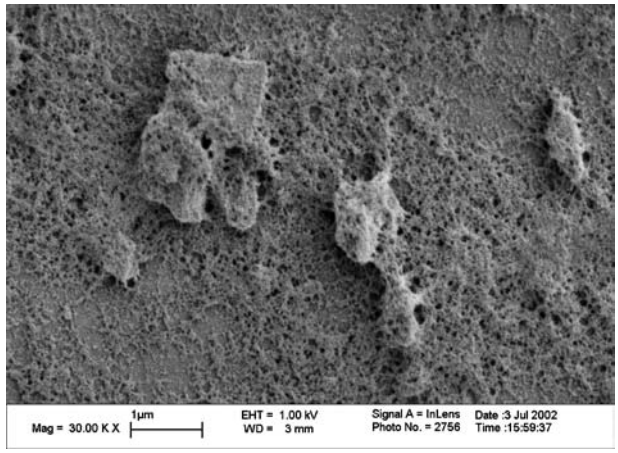

Figure 8 The same fracture surface as in Fig. 7 at higher magnification showing the porous aerogel structure between the sand grains.

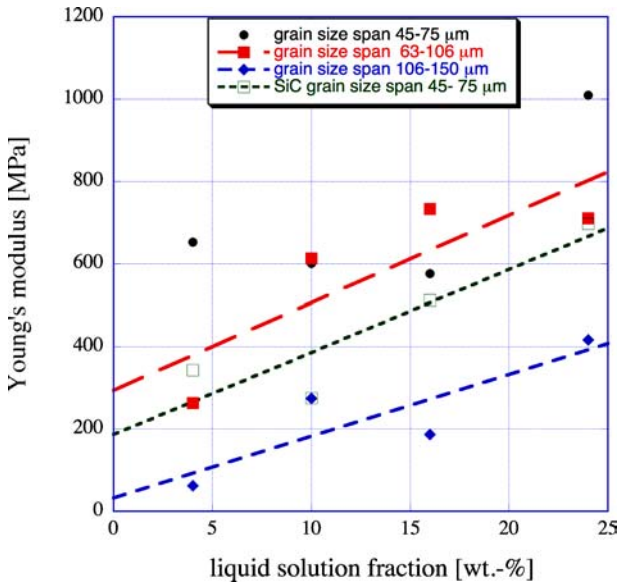

Figure 9 Elastic modulus versus sol fraction.

The elastic modulus depends mainly on the aerogel content and to a lesser extent on the sand type. A few results are shown in Fig. 9. The elastic modulus varies in a linear manner with the RF sol fraction as expected from a simple rule of mixtures. The aerogel mainly dictates its values.

4. Discussion

Sand binder systems are widely used in foundry practice. Polymeric binders like furan resins, polyurethane, phenolic resins are commonly used. Due to ecological and economic considerations the amount of binder constantly was reduced in the last decade. Typically in todays foundry practice sands, and most often quartz sand is used, are bonded with less than one weight percent binding resin. The strength obtained with these sand-binder systems range from 1–2 N/mm^2 using the cold-box process, the Croning process leads to materials with 0.4

to 14 and the hot-box to strengths between 4–9 N/mm^2 [8]. The RF-aerogel binder leads to similar bending and compression strength especially at high solution contents. It seems that compared to conventional binder systems the amount of 10, 16 or 24 wt% aerogel solution is huge. It has, however, to be noticed that this is the amount of liquid solution. After drying the amount of solid binder is smaller by a factor of approximately 3, meaning that 10 wt% RF-solution leads to 3 wt% RF-aerogel binder.

The results of the mechanical test described above can be summarized as

- the smaller the grain size of the sand the higher the compression and bending strength
- with increasing amount of aerogel the strength increases
- the rougher the sand surface the higher the strength.

These observation can be explained qualitatively with a simple extension of the classical Griffith criterion for brittle solids [11]. This criterion has the simple form

$$\sigma_F = \left(\frac{2E'\gamma}{\pi c_0}\right)^{1/2} \tag{1}$$

with σ_F the fracture stress, c_0 the initial crack length, γ the surface tension of the solid and E' is the modulus being different under plane stress or plane strain loading conditions. This criterion has to be modified to take into account the composite nature of the AeroSands and the fracture path.

In an AeroSand the fracture follows the interface between the sand grains and the aerogel network and of course to a smaller extent the aerogel bridges between the grains are directly broken. Let the interface tension between sand and the polymeric aerogel be γ_{SA}. This interface tension does, however, not enter directly into the Griffith criterion, since the aerogel has its own porosity such that the sand grains are not enclosed by a dense polymer but only touched at points or a small area of their surface. The occupied area of a sand grain is calculated as follows. Let ϵ_A be the porosity of the aerogel. If R_A is the radius of a particle the aerogel is made of and let λ be the average distance between to particles in the network, then the porosity can be expressed as $\epsilon_A = 1 - {R_A}^3/(R_A + \lambda/2)^3$. Solving this equation for λ and using $D_A = 2\,R_A$ we obtain

$$\lambda = D_A\left[\left(\frac{1}{1-\epsilon_A}\right)^{1/3} - 1\right]. \tag{2}$$

The coverage ζ of the sand grains is now obtained from

$$\zeta = \left(\frac{D_A}{\lambda}\right)^2 f_A\,, \tag{3}$$

where f_A is the fraction of pore volume in the sand bed filled by the aerogel sol. This factor is defined by the pore volume fraction of the sand ϵ_S and the ratio $\Phi_A = V_{\text{sol}}/V_{\text{total}}$ with V_{sol} the volume of the solution and V_{total} the total volume of the aerosand mixture as $f_A = \Phi_A/\epsilon_S$.

We can now replace the interface tension by a modified expression, namely $\gamma_{SA}\zeta$. Insertion into the Griffith criterion yields the final result if we suppose that initially crack lengths exists of the order of the sand grain size, namely $c_0 = \alpha\, D_S$, with α an arbitrary factor of porportionality of the order 1,

$$\sigma_F^{\text{AeroSand}} = \sigma_0\sqrt{\frac{\Phi_A}{D_S}}\,, \tag{4}$$

with

$$\sigma_0 = \frac{1}{(\frac{1}{1-\epsilon_A})^{1/3} - 1}\sqrt{\frac{2E'\gamma_{SA}}{\alpha\pi\epsilon_S}}\,. \tag{5}$$

The equation describes qualitatively the observation stated above in the summary. In order to test the trends given by this equation we plotted the data given before in the tables. Although Equation 4 requires to use the volume fraction of dry aerogel, we use the technically easier to measure and experimentally useful weight percent fraction. Calculating the relation between weight and volume fraction in the aerosands fortunately shows that in the range of weight fraction used in our experiments there is a linear relation between both. Thus using weight fraction instead of volume fraction does not change the functional dependence of Equation 4. Figs 10 and 11 both show the modified Griffith criterion fits to the experimental values.

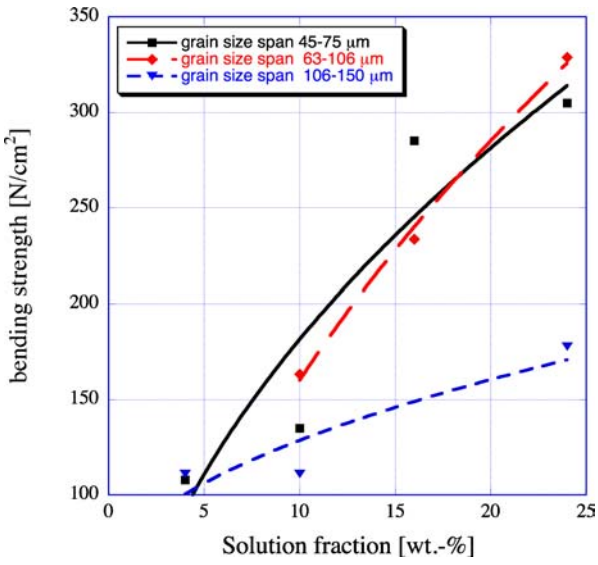

Figure 10 Bending strength of AeroSands made with Alodur$^{\text{TM}}$ as it varies with solution content. The drawn in curves are fits according to the theoretical expression of Equation 4.

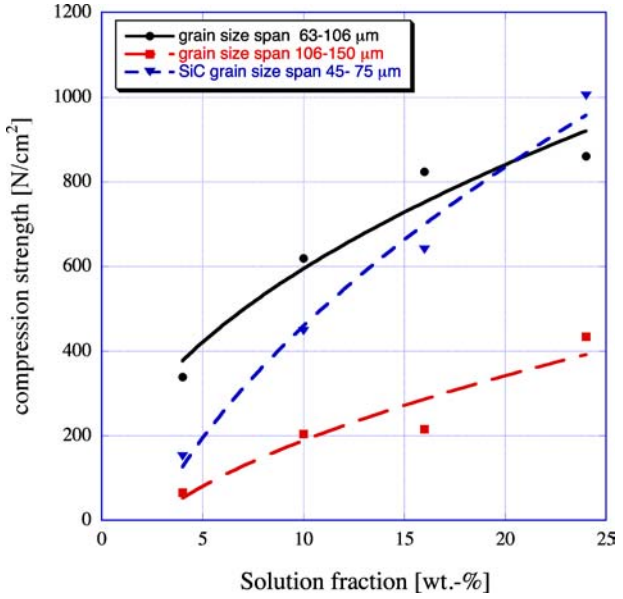

Figure 11 Compression strength of AeroSands made with Alodur™ as it varies with solution contents. The drawn in curves are fits according to the theoretical expression of Equation 4.

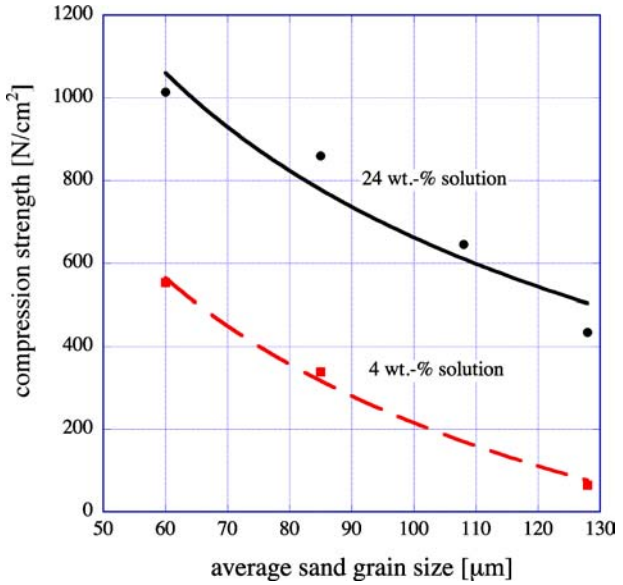

Figure 12 Compression strength of AeroSands made with Alodur™ as it varies with grain size for two different solution contents. The drawn in curves are fits according to the theoretical expression of Equation 4.

The same is true for the dependence on grain size, where a fit was made to the values and plotted in Fig. 12.

The agreement between experimental values and theoretical explanation should not be taken too seriously but just looked at as a trend. The modified Griffith criterion then gives hints, how to improve the strength. The observation that a rougher sand surface binds better with the aerogel can be explained qualitatively, since then the crack has to open a much larger area compared to a smooth interface. One could take this into account in the Griffith criterion by multiplying the interface tension with a sand surface roughness factor r_S, $1 \leq r_S < \infty$. The observation that both sands containing silicondioxide exhibit very low strength values may be explained by a modification of the gelation process of the embedding aerogel solution. It is well known that quartz always has OH groups adsorbed at its surface. This could lead to a locally modification of the gelation kinetics, since these OH groups modify the pH value. If this would be true one would obtain at the interface between quartz grains and the RF solution an aerogel being different than that formed under pure conditions mentioned above. The polymeric particles would become smaller, the network more open. In addition during drying the network would than locally collapse leading to loosely bonded sand grains and thus a low composite strength.

5. Conclusion

RF-Aerogels can bind foundry sands the better the larger the aerogel amount. The strength levels are comparable to conventional binder systems. The advantages of the AeroSands described in the introduction, especially concerning aspects of easy core removal, are not payed off by a loss in strength. The mechanical properties can be explained using a simple extension of the Griffith criterion and a mixture rule for the elastic modulus.

References

1. L. RATKE, S. AHRWEILER, S. BRÜCK, S. SOUS and D. TSCHEUSCHNER, in Proc. International Conf. on Solidification and Processing, Bangalore 2001, edited by B. K. Dhindaw, B. S. Murty, S. Sen (Science Publishers, Enfield 2001) p. 183.
2. S. BRÜCK and L. RATKE, EUROMAT 2001, Conference Proceedings, Rimini, 10–14 July 2001 Organised by Associazione Italiana di Metallurgia, Symposium on Solidification, ISBN 88-85298-39-7. Paper no. 260, p. 9.
3. S. BRÜCK and L. RATKE, *J. Sol-Gel Sci.* **26** (2003) 663.
4. S. BRÜCK, *Giessereipraxis* **9** (2002) 343.
5. J. THIEL, H. KLEIN, S. BRÜCK and L. RATKE, *GIT Labor Fachzeitschrift* **47** (2003) 162.
6. A. D. BUSBY and M. R. STANCLIFFE, *Foundryman* February (1997), 37.
7. R. PETRICEVIC, G. REICHENAUER, V. BOCK, A. EMMERLING and J. FRICKE, *J. Non-Cryst. Sol.* **225** (1998) 4145.
8. W. TILCH and E. FLEMMING, "*Formstoffe und Formverfahren*" (Dt. Verlag fÿr Grund-stoffindustrie Leipzig/Stuttgart, 1993).
9. J. MCD. B. BROWN, "Introductory Solid Mechanics" (J. Wiley and Sons, London, 1973).
10. U. POHL, *Herstellung und Charakterisierung von ultraleichten Aerogelverbundwerkstoffen*, Batchelor thesis, Technical university of Aachen, 2004.
11. B. LAWN, "Fracture of Brittle Solids" - 2 edn. (Cambridge University Press, Cambridge 1993).

Received 25 February 2004
and accepted 13 April 2005